Coverage and Rate Analysis of Mega-Constellations Under Generalized Serving Satellite Selection

Niloofar Okati and Taneli Riihonen
Faculty of Information Technology and Communication Sciences, Tampere University, Finland
e-mail: {niloofar.okati, taneli.riihonen}@tuni.fi

2022 IEEE Wireless Communications and Networking Conference (WCNC) | 978-1-6654-4266-4/22/$31.00 ©2022 IEEE | DOI: 10.1109/WCNC51071.2022.9771936

***Abstract*—The dream of having ubiquitous and high-capacity connectivity is coming true by emerging low Earth orbit (LEO) Internet constellations through several commercial plans, e.g., Starlink, Telesat, and Oneweb. The analytical understanding of these networks is crucial for accurate network assessment and, consequently, acceleration in their design and development. In this paper, we derive the coverage probability and the data rate of a massive LEO network under arbitrarily distributed fading and shadowing. The conventional user association techniques, based on the shortest distance between the ground terminal and the satellite, result in a suboptimal performance of the network since the signal from the nearest server may be subject to severe shadowing due the blockage by nearby obstacles surrounding the ground terminal. Thus, we take into account the effect of shadowing on the serving satellite selection by assigning the ground terminal to the satellite which provides the highest signal-to-noise ratio at the terminal's place, resulting in a more generalized association technique, namely the best server policy (BSP). To maintain tractability of our derivations and consider the latitude-dependent distribution of satellites, we model the satellites as a nonhomogeneous Poisson point process. The numerical results reveal that implementing the BSP for serving satellite selection leads to significantly better performance compared to the conventional nearest server policy (NSP).**

I. Introduction

Low Earth orbit (LEO) Internet constellations are gaining increasing popularity all around the world due to providing seamless connectivity, especially for isolated regions where deployment of terrestrial networks is not economically feasible or for countries with restricted access to Internet. To keep pace with the commercial progress of LEO networks and accelerate their development, analytical modeling and understanding of these networks — without time consuming and network-specific orbital simulations — are of great importance.

Although several aspects of massive LEO constellations have been investigated recently in the literature [1]–[10], little attention was paid to the effect of shadowing on the selection of the serving satellite, which noticeably affects the network performance. The server association used in the literature is based on the shortest distance, i.e., the so-called the *nearest server policy* (NSP), which is the most simplistic association technique and is rarely used in practice since it is unable to include the effect of the large-scale attenuation, i.e., shadowing, on the variation of the received signal. In this work, we will implement the more realistic association technique, the *best server policy* (BSP), which includes the shadowing effect on the serving satellite selection by assigning the ground terminal to a satellite that provides the highest signal-to-noise ratio (SNR) at the terminal's place.

The best server policy is frequently used to evaluate the performance of terrestrial networks [11]–[13], and proved to provide more reliable network performance. Moreover, the best server policy is more in line with practical association techniques since, in reality, the SNR at the receiver is a major criterion to determine the server [13].

The literature on LEO network analysis has been mostly limited to simulation-based deterministic analyses [14]–[16] until recently that the application of stochastic geometry and statistical models for tractable analysis of massive wireless networks [17]–[22] was extended to LEO networks' analysis. Utilization of stochastic geometry enables characterization of the serving distance which is a key parameter in performance evaluation of theses networks. However, the serving distance for analytical modeling of LEO networks is mostly assumed be to the shortest distance between the user and the satellites.

In [1], we derived the coverage probability and the data rate of a massive LEO network in presence of co-channel interference by modeling the network as a binomial point process (BPP). Since the satellites' locations in actual constellations barely follow a uniform distribution, we adjusted the inherent performance mismatch numerically in [1]. The mismatch was also compensated in [2] and [3] through analytically finding the effective number of satellites for every user's latitude and modeling the network as a nonhomogeneous Poisson point process (PPP) with a latitude-dependent intensity, respectively. Unlike [1], [2], shadowing was included in the propagation model in [3], but it had no effect on the association rule and the user connects to its nearest satellite. A more generalized system model was studied by inclusion of interference in [4].

The contact angle, i.e., the minimum angular distance between the satellites and the user, is characterized in [5] to evaluate the performance of a LEO network without considering the effect of shadowing attenuation. The results were then used in [6] to find the altitude that maximizes coverage probability. The uplink performance of a LEO network in presence of terrestrial interferers was characterized in [7]. In [10], the distribution of conditional coverage probability was derived, given the nodes' positions, for a satellite–terrestrial relay network in order to evaluate the percentage of ground users that may reach a target SINR threshold.

In [8], essential distance distributions were formulated for LEO networks assuming satellites are distributed on multiple concentric spheres, each of which has a known specific radius. The results were then used to analyze the coverage probability in [9] when satellite gateways relay the data between the satellites and the terrestrial users. Despite assuming shadowed Rician channels in [9], [10], they had no effect on the contact distances.

According to the literature review, the best server policy has not yet been characterized for analytical evaluation of LEO networks, in spite of the fact that it is the most frequently used association technique in practice. Moreover, the shadowing effect, which enables the characterization of the best server policy, was not considered in most of the literature.

In this paper, we formulate new analytical expressions to evaluate the coverage probability and rate of a LEO network, assuming that the server is selected based on the best server policy. Including shadowing in the propagation model, we assume that the ground terminal associates with the satellite that provides the highest received SNR for the terminal. We corroborate our derivations through Monte Carlo simulations, and compare them with the conventional nearest server policy, which was presented in [3]. As our numerical results illustrate, the best server policy results in significantly better performance in both coverage probability and data rate compared with the nearest server policy.

The remainder of this paper is organized as follows. Section II introduces the studied system model and the mathematical preliminaries to model a LEO network as a nonhomogeneous PPP. Distance distributions required to characterize the coverage probability and the data rate of a LEO network are presented in Section III. The numerical results are provided in Section IV. Finally, the paper is concluded in Section V.

II. System Model

In this section, firstly, we describe the actual LEO constellation that will be studied in this paper. Secondly, we present the (re)modeled nonhomogeneous PPP which not only captures all the characteristics of the actual physical network, but also enables us to tractably analyze and derive the network performance metrics. One should note that the study holds for both downlink and uplink directions equivalently although some of the following system aspects are specified from the downlink perspective for simplicity.

The actual network studied in this paper is a massive LEO Internet constellation, as shown in Fig. 1, consisting of N satellites which are distributed uniformly on circular orbits at a given altitude, $r_{\min}$. The orbital planes are all inclined to an angle, denoted by ι. The ground terminals (GTs), i.e., users and/or gateways, are located on Earth's surface at an arbitrary latitude denoted by ϕ_{u}. Earth is assumed to be a perfect sphere with radius $r_\oplus \approx 6371$ km.

A satellite is visible to a ground terminal, i.e., it can receive from or transmit to it, if it is elevated above the user's horizon to a minimum angle of $\theta_{\min}$. The distances from the satellites to the ground terminal, their corresponding channel gains, and the shadowing coefficients are denoted by R_n, G_n, and $\mathcal{X}_n$, where $n = 0, 1, \ldots, N-1$. Throughout the paper, we reserve

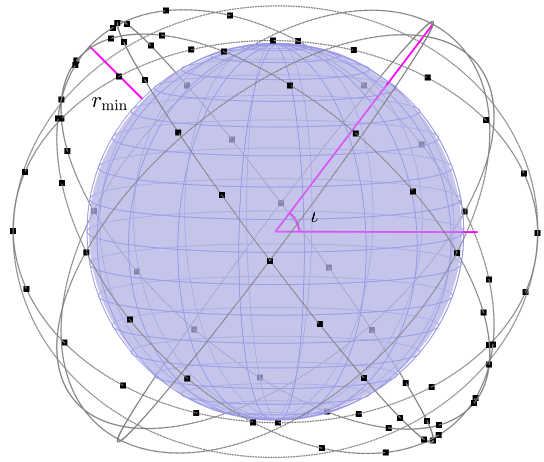

Fig. 1. A LEO constellation in an example case of $N = 1000$ satellites flying on $\iota = 53°$ inclined orbits at $r_{\min} = 1800$ km. Only 6 example orbital planes are shown for clarity.

index zero for the serving link, i.e., R_0, G_0, and $\mathcal{X}_0$ represent the distance to the server, its corresponding fading gain and its shadowing coefficient, respectively. A satellite and GT may be able to communicate only if $R_n \leq r_{\max}$, where $r_{\max}$ is the distance between the satellite and GT when the satellite is at the minimum elevation angle, i.e., $\theta_{\min}$. Obviously, $r_{\max}$ is a function of $\theta_{\min}$ and is given as [3]

$$\frac{r_{\max}}{r_\oplus} = \sqrt{\frac{r_{\min}}{r_\oplus}\left(\frac{r_{\min}}{r_\oplus}+2\right)+\sin^2(\theta_{\min})} - \sin(\theta_{\min}). \quad (1)$$

The signal-to-noise ratio at the receiver, based on the above system model, can be expressed as

$$\mathrm{SNR} = \begin{cases} \dfrac{p_{\mathrm{s}} G_0 \mathcal{X}_0 R_0^{-\alpha}}{\sigma^2}, & R_0 \leq r_{\max}, \\ 0, & \text{otherwise}, \end{cases} \quad (2)$$

where p_{s} is the constant transmission power. The parameter $\alpha = 2$ is a path loss exponent and the power of the additive noise is denoted by σ^2.

In this paper, we implement the best server policy to select the serving satellite. Accordingly, the serving satellite will be the one which provides the strongest SNR for the receiver. Since fading coefficients, G_n, vary quickly over the time, we assume that they have no effect on the association technique. Therefore, when implementing the best server policy, the serving link must satisfy the following equation:

$$\mathcal{X}_0^{-\frac{1}{\alpha}} R_0 = \min_n \left(\mathcal{X}_n^{-\frac{1}{\alpha}} R_n | R_n < r_{\max}\right). \quad (3)$$

We then remodel the actual network, described earlier, as a nonhomogeneous PPP which allows us to take into account the varying density of satellites along different latitudes while maintaining the tractability of our derivations [3]. Ergo, we assume that the satellites are distributed according to a nonhomogeneous PPP, on a spherical shell with radius $r_\oplus + r_{\min}$.

By the definition of a nonhomogeneous PPP, the number of points in some bounded region $\mathcal{A}$ of the orbital shell is a Poisson-distributed random variable denoted by $\mathcal{N}$. Thereby, the probability to have n satellites in $\mathcal{A}$ is given by

$$P_n(\mathcal{A}) \triangleq \mathbb{P}(\mathcal{N}=n) \tag{4}$$
$$= \frac{1}{n!}\left(\iint_{\mathcal{A}} \delta(\phi_{\rm s},\lambda_{\rm s})\,(r_{\min}+r_\oplus)^2 \cos(\phi_{\rm s})\, d\phi_{\rm s} d\lambda_{\rm s}\right)^n$$
$$\times \exp\left(-\iint_{\mathcal{A}} \delta(\phi_{\rm s},\lambda_{\rm s})\,(r_{\min}+r_\oplus)^2 \cos(\phi_{\rm s})\, d\phi_{\rm s} d\lambda_{\rm s}\right),$$

where $\delta(\phi_{\rm s},\lambda_{\rm s})$ is the intensity function of nonhomogeneous PPP at latitude $\phi_{\rm s}$ and longitude $\lambda_{\rm s}$. Based on the given system model, $\mathcal{A}$ is any spherical cap in the area where visible satellites to the user exist.

The intensity of nonhomogeneous PPP, when satellites are distributed uniformly on inclined low Earth orbits, is a function the satellites' latitudinal element, $\phi_{\rm s}$, which is characterized in [3] as

$$\delta(\phi_{\rm s},\lambda_{\rm s}) = \delta(\phi_{\rm s}) \tag{5}$$
$$= \frac{N}{\sqrt{2}\pi^2 (r_{\min}+r_\oplus)^2 \sqrt{\cos(2\phi_{\rm s}) - \cos(2\iota)}}.$$

As implied above, the intensity is inherently independent of the satellites' longitudinal element, $\lambda_{\rm s}$.

III. Performance Analysis

In this section, we find mathematical expressions for the coverage probability and the data rate of the described LEO constellation under the best server policy. Modeling the satellites locality as a nonhomogeneous PPP, we are able to find the distance distributions, in terms of their cumulative distribution function (CDF) and probability density function (PDFs), which will contribute to arriving at our main derivations in this paper, i.e., coverage probability and data rate.

A. Distance Distributions

In the following lemma, we derive the distribution of the distance from the user to any visible satellite, $R_n^{\rm vis}$, in terms of its CDF.

Lemma 1. *The CDF of the distance from any visible satellite in the constellation $R_n^{\rm vis}$ to the ground terminal is given by*

$$F_{R_n^{\rm vis}}(r_n) \triangleq \mathbb{P}(R_n < r_n | R_n < r_{\max}) \tag{6}$$
$$= \frac{\iint_{\mathcal{A}(r_n)} \delta(\phi_{\rm s},\lambda_{\rm s})\,(r_{\min}+r_\oplus)^2 \cos(\phi_{\rm s})\, d\phi_{\rm s} d\lambda_{\rm s}}{\iint_{\mathcal{A}(r_{\max})} \delta(\phi_{\rm s},\lambda_{\rm s})\,(r_{\min}+r_\oplus)^2 \cos(\phi_{\rm s})\, d\phi_{\rm s} d\lambda_{\rm s}}$$

for $r_{\min} \le r_n \le r_{\max}$. $\mathcal{A}(r_n)$ and $\mathcal{A}(r_{\max})$ are the cap area where all satellites therein have a distance less than or equal to r_n and $r_{\max}$ to the GT, respectively.

Proof. The CDF of the distance from any visible satellite to the GT is equal to the CDF of surface integral of $\delta(\phi_{\rm s},\lambda_{\rm s})$ over the spherical cap $\mathcal{A}(r_n)$. Conditioning on the visibility, the CDF is trivially calculated as in (6). □

Corollary 1. *The CDF of $R_n^{\rm vis}$, when the satellites are distributed according to a nonhomogeneous PPP with a latitude-dependent intensity, $\delta(\phi_{\rm s})$, is*

$$F_{R_n^{\rm vis}}(r_n) \tag{7}$$
$$= \frac{\int_{\max(\phi_{\rm u}-\theta(r_n),-\iota)}^{\min(\phi_{\rm u}+\theta(r_n),\iota)} \delta(\phi_{\rm s})\cos(\phi_{\rm s})\cos^{-1}\left(\frac{\cos(\theta)}{\cos(\phi_{\rm s}-\phi_{\rm u})}\right) d\phi_{\rm s}}{\int_{\max(\phi_{\rm u}-\theta(r_{\max}),-\iota)}^{\min(\phi_{\rm u}+\theta(r_{\max}),\iota)} \delta(\phi_{\rm s})\cos(\phi_{\rm s})\cos^{-1}\left(\frac{\cos(\theta)}{\cos(\phi_{\rm s}-\phi_{\rm u})}\right) d\phi_{\rm s}},$$

where $\theta(r) = \cos^{-1}\left(1 - \frac{r^2 - r_{\min}^2}{2(r_{\min}+r_\oplus)r_\oplus}\right)$ is the polar angle difference between a satellite and the ground terminal.

Proof. Corollary is obtained by calculating the longitude range inside the spherical cap and with the aid of the basic geometry (for more details see [3, Lemma 2]), and substitution in Lemma 1. □

Considering the effect of shadowing on BSP association, let us define $\tilde{R}_0 \triangleq \min_n \mathcal{X}_n^{-\frac{1}{\alpha}} R_n^{\rm vis}$ as *the nearest effective distance* from the visible satellites to the user. The following lemma gives the PDF distribution of $\tilde{R}_0$.

Lemma 2. *The PDF of the nearest effective distance $\tilde{R}_0$ is given by*

$$f_{\tilde{R}_0}(\tilde{r}_0) = \sum_{n=0}^{\infty} n P_n(\mathcal{A}(r_{\max}))$$
$$\times \int_0^\infty \alpha z_n^{-\alpha-1} f_{\mathcal{X}_n}\left(z_n^{-\alpha}\right) F_{R_n^{\rm vis}}\left(\frac{\tilde{r}_0}{z_n}\right) d_{z_n}$$
$$\times \left(1 - \int_0^\infty \alpha z_n^{-\alpha-1} f_{\mathcal{X}_n}\left(z_n^{-\alpha}\right) F_{R_n^{\rm vis}}\left(\frac{\tilde{r}_0}{z_n}\right) d_{z_n}\right)^{n-1}, \tag{8}$$

where the PDF of the random variable $\mathcal{Z}_n \triangleq \mathcal{X}_n^{-\frac{1}{\alpha}}$ is evaluated at point z_n.

Proof. See Appendix A. □

If satellites were distributed according to a homogeneous PPP with constant density $\delta = \frac{N}{4\pi(r_{\min}+r_\oplus)^2}$, the distribution of the nearest effective distance would be simplified as in the following lemma. This requires compensating for the density mismatch by replacing N by the effective number of satellites.

Lemma 3. *The PDF of the nearest effective distance $\tilde{R}_0$ when the satellites are distributed uniformly with constant intensity, $\delta = \frac{N}{4\pi(r_{\min}+r_\oplus)^2}$, is*

$$f_{\tilde{R}_0}(\tilde{r}_0) = \sum_{n=0}^{\infty} \frac{1}{(n-1)!}\left(\frac{\delta\pi\left(r_{\max}^2 - r_{\min}^2\right)}{1 - \frac{r_{\min}}{r_\oplus + r_{\min}}}\right)^n$$
$$\times \exp\left(-\frac{\delta\pi\left(r_{\max}^2 - r_{\min}^2\right)}{1 - \frac{r_{\min}}{r_\oplus + r_{\min}}}\right)$$
$$\times \left(1 - \int_0^\infty \alpha z_n^{-\alpha-1} f_{\mathcal{X}_n}\left(z_n^{-\alpha}\right)\left(\frac{\left(\frac{\tilde{r}_0}{z_n}\right)^2 - r_{\min}^2}{r_{\max}^2 - r_{\min}^2}\right) d_{z_n}\right)^{n-1}$$
$$\times \int_0^\infty \alpha z_n^{-\alpha-3} f_{\mathcal{X}_n}\left(z_n^{-\alpha}\right)\left(\frac{2\tilde{r}_0 - r_{\min}^2}{r_{\max}^2}\right) d_{z_n}. \tag{9}$$

TABLE I
SIMULATION PARAMETERS

Parameters	Values
Path loss exponent, α	2
Rician factor, K	10
Transmit power, p_{s}	50 dBm
Noise power, σ^2	-120 dBm
Frequency	13.5 GHz
Mean and standard deviation of lognormal distribution: μ_{s}, σ_{s}	0 dB, 9 dB

Proof. Since the intensity function δ is constant, $P_n\left(\mathcal{A}\left(r_{\max}\right)\right)$ is obtained simply by multiplying δ by the surface of the spherical cap, $\mathcal{A}\left(r_{\max}\right)$, where the visible satellites can reside. Using Lemma 1, we have $F_{R_n^{\text{vis}}}\left(\frac{\tilde{r}_0}{z_n}\right) = \frac{\mathcal{A}\left(\frac{\tilde{r}_0}{z_n}\right)}{\mathcal{A}(r_{\max})} = \frac{\left(\frac{\tilde{r}_0}{z_n}\right)^2 - r_{\min}^2}{r_{\max}^2 - r_{\min}^2}$, since the density is constant over the spherical shell. □

B. Coverage Probability

In this subsection, we utilize the distance distributions obtained in the previous section to derive the coverage probability of a LEO constellation for an arbitrarily located ground terminal under the best server policy. The coverage probability is the probability of having a greater SNR than a minimum threshold, $T > 0$, at the receiver. In other words, whenever the received SNR is above the threshold level, the receiver is considered to be within the coverage and the data is transmitted successfully.

Proposition 1. *The probability of network coverage for an arbitrarily located GT, under generally distributed fading and shadowing as well as BSP association is*

$$P_{\mathrm{c}}\left(T\right) \triangleq \mathbb{P}\left(\mathrm{SNR} > T\right) = \int_0^\infty \left(1 - F_{G_0}\left(\frac{T \tilde{r}_0^\alpha \sigma^2}{p_{\mathrm{s}}}\right)\right) f_{\tilde{R}_0}(\tilde{r}_0) d\tilde{r}_0, \quad (10)$$

where $F_{G_0}(\cdot)$ is the CDF of the channel gain G_0 and $f_{\tilde{R}_0}(\tilde{r}_0)$ is given in Lemmas 2 and 3.

Proof. To obtain (10), we start with the definition of coverage probability:

$$\begin{aligned} P_{\mathrm{c}}\left(T\right) &= \mathbb{E}_{\tilde{R}_0}\left[\mathbb{P}\left(\mathrm{SNR} > T | \tilde{R}_0\right)\right] \\ &= \int_0^\infty \mathbb{P}\left(\mathrm{SNR} > T | \tilde{R}_0 = \tilde{r}_0\right) f_{\tilde{R}_0}\left(\tilde{r}_0\right) dr_0 \\ &= \int_0^\infty \mathbb{P}\left(G_0 > \frac{T \tilde{r}_0^\alpha \sigma^2}{p_{\mathrm{s}}}\right) f_{\tilde{R}_0}\left(\tilde{r}_0\right) dr_0, \end{aligned} \quad (11)$$

The proof is completed by substituting the complementary CDF of G_0. □

Note that the effect of the shadowing distribution in the coverage probability is embedded in the PDF of the nearest effective distance, $f_{\tilde{R}_0}\left(\tilde{r}_0\right)$, given in Lemmas 2 and 3.

C. Average Data Rate

Let us then turn to the average achievable data rate (in bits per channel use), which states the ergodic capacity derived from the Shannon–Hartley theorem over a fading communication link normalized to unit bandwidth.

Proposition 2. *The average rate (in bits/s/Hz) of an arbitrarily located GT, under BSP association, and generally distributed fading and shadowing is*

$$\bar{C} \triangleq \mathbb{E}\left[\log_2\left(1 + \mathrm{SNR}\right)\right] = \int_0^\infty \int_0^\infty \log_2\left(1 + \frac{p_{\mathrm{s}} g_0 \tilde{r}_0^{-\alpha}}{\sigma^2}\right) f_{G_0}(g_0) f_{\tilde{R}_0}\left(\tilde{r}_0\right) \, dg_0 \, d\tilde{r}_0, \quad (12)$$

where $f_{G_0}(g_0)$ represents the PDF of channel gain G_0 and $f_{\tilde{R}_0}(\tilde{r}_0)$ is given in Lemmas 2 and 3.

Proof. Taking the expectation over the serving distance and the channel gain, we have

$$\begin{aligned} \bar{C} &= \mathbb{E}_{G_0, R_0}\left[\log_2\left(1 + \mathrm{SNR}\right)\right] \\ &= \int_0^\infty \mathbb{E}_{G_0}\left[\log_2\left(1 + \frac{p_{\mathrm{s}} G_0 \tilde{r}_0^{-\alpha}}{\sigma^2}\right)\right] f_{\tilde{R}_0}\left(\tilde{r}_0\right) d\tilde{r}_0. \end{aligned} \quad (13)$$

The inner integral comes from the expectation w.r.t. G_0. □

IV. NUMERICAL RESULTS

In this section, we evaluate and compare the effect of the two association policies, i.e., the best server policy (BSP) which is analyzed above in this paper and the nearest server policy (NSP) in [3], on the performance of a LEO network. We also corroborate our analytical derivations through Monte Carlo simulations on the actual constellations.

Since most of the signal path is through the free space, we set the path loss exponent to $\alpha = 2$. The small-scale fading around the GT is assumed to be Rician with parameter $K = 10$. The CDF and the PDF of G_0, required to evaluate Propositions 1 and 2, are

$$F_{G_0}(g_0) = 1 - Q_1\left(\sqrt{2K}, \sqrt{g_0}\right) \quad (14)$$

and

$$f_{G_0}(g_0) = \frac{1}{2} e^{-\frac{g_0 + 2K}{2}} I_0\left(\sqrt{2K g_0}\right), \quad (15)$$

respectively, where $Q_1(\cdot,\cdot)$ denotes the Marcum Q-function and $I_0(\cdot)$ is the modified Bessel function of the first kind. Shadowing is assumed to have a lognormal distribution which is represented as $\mathcal{X}_0 = 10^{X_0/10}$ such that X_0 has a normal distribution with mean $\mu_{\mathrm{s}} = 0$ and standard deviation $\sigma_{\mathrm{s}} =$ 9 dB. Thus, the PDF of lognormal shadowing is

$$f_{\mathcal{X}_0}(x_0) = \frac{10}{\ln(10)\sqrt{2\pi}\sigma_{\mathrm{s}} x_0} \exp\left(-\frac{1}{2}\left(\frac{10\log_{10}(x_0) - \mu_{\mathrm{s}}}{\sigma_{\mathrm{s}}}\right)^2\right). \quad (16)$$

The ground terminal is located on 25° latitude. The transmit power and the noise power are set to 50 dBm and -120 dBm, respectively. The operating frequency is assumed to be 13.5 GHz. For the reference simulated constellation, satellites are placed uniformly on circular orbits centered at Earth's center with radius $r_\oplus + r_{\min}$. Table I summarizes the simulation parameters used to generate the numerical results.

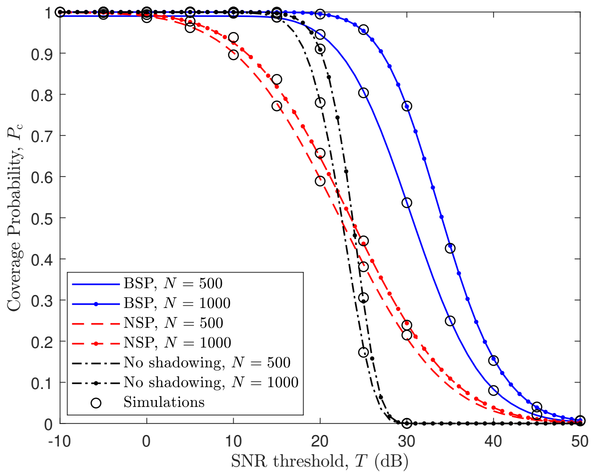

Fig. 2. Verification of Proposition 1 with simulations when $K = 10$, $\phi_u = 25°$, $\iota = 53°$, $r_{\min} = 500$ km, and $\theta_{\min} = 10°$. The lines and the markers represent the analytical results and simulations, respectively.

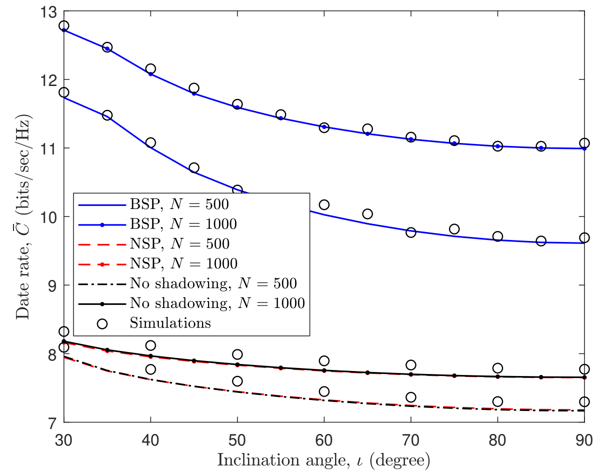

Fig. 3. Data rate versus inclination angle when $K = 10$, $\phi_u = 25°$, $r_{\min} = 500$ km, and $\theta_{\min} = 10°$. The lines and the markers represent the analytical results and simulations, respectively.

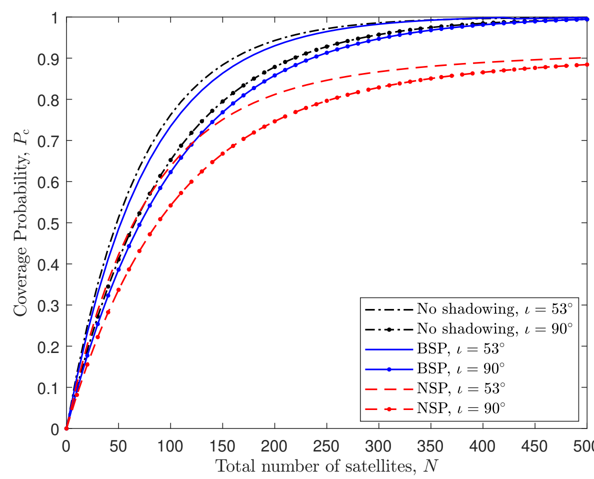

Fig. 4. Coverage probability versus constellation size when $T = 10$ dB, $K = 10$, $\phi_u = 25°$, $\iota = 53°$, $r_{\min} = 500$ km, and $\theta_{\min} = 10°$.

Figure 2 depicts the coverage probability versus SNR threshold for BSP, NSP, and non-shadowing environment for $N = 500$ and 1000 satellites. A fair match between the theory (plotted by lines) and the simulations (plotted by markers) is observed in the figure. As can be seen in the figure, the BSP results in a significantly better coverage probability compared to NSP, since the overall SNR at the receiver is improved by inclusion of shadowing in association policy. It is obvious that when shadowing is assumed to be zero, the two association techniques become the same.

The same as for the coverage probability, the BSP provides more reliable data rate compared to the NSP as shown in Fig. 3. We verify the expression given in Proposition 2 (depicted with lines) with simulations (depicted with markers). The data rate slightly decreases with increasing the inclination angle since the satellites' density decreases accordingly. Larger constellation size results in higher data rates due to more chance of being connected to the best possible server.

The effect of constellation size on coverage probability for BSP and NSP association techniques and two inclination angles of $\iota = 53°$ and $\iota = 90°$ are illustrated in Fig. 4. The SNR threshold is set to 10 dB. As expected, BSP shows a superior performance compared to NSP and the performance difference rises with increasing the constellation size. Smaller inclination angles result in higher coverage probability due to providing a higher density for a given number of satellites, especially when the constellation size is not too large. As the number of satellites exceeds a certain limit, the coverage probability saturates to a certain value, implying that increasing the constellation size does not always improve the performance (i.e., no better serving channel can be associated).

The data rate for different total number of satellites and inclination angles is depicted in Fig. 5. The curves follow the same behaviour as those in Fig. 4, which illustrates the better performance of BSP. As can be seen, when $\sigma_s = 9$ dB, the effect of shadowing on NSP association is insignificant. Thus, we skipped plotting the results for non-shadowing case in Fig. 5 since they overlap the results of NSP.

V. Conclusions

In this paper, the best server policy to assign a ground terminal to the best LEO satellite, which provides the highest SNR at the receiver, is studied and compared with conventional association techniques that only consider the distance between transceivers. Utilizing a nonhomogeneous Poisson point process to model the satellites' locality, enabled us to tractably analyze a LEO network for its two main performance metrics, i.e., the coverage probability and the data rate, while precisely capturing the characteristics of the actual physical network. As a result, the distribution of the serving distance based on BSP is derived mathematically which is a crucial parameter in network performance assessment. From the nu-

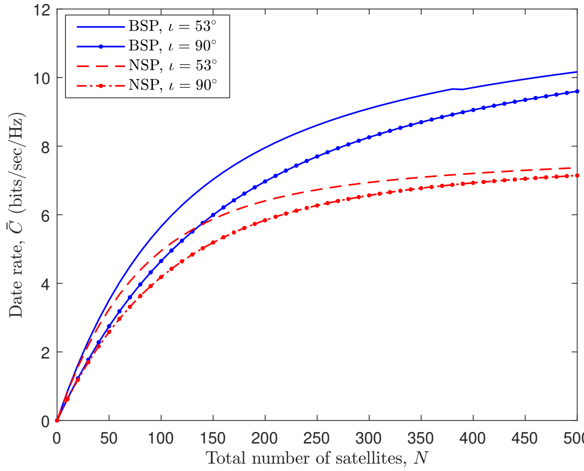

Fig. 5. Data rate versus constellation size when $K = 10$, $\phi_{\rm u} = 25°$, $r_{\min} = 500$ km, and $\theta_{\min} = 10°$.

merical results, other than verification of our derivations, we presented the coverage probability and the data rate in terms of different network parameters, e.g., inclination angle and the constellation size. The best serving policy resulted in a significantly better performance compared to the conventional nearest server policy for different network parameter settings.

Appendix

A. Proof of Lemma 2

The CDF of $\tilde{R}_0$ is defined as

$$
\begin{aligned}
&F_{\tilde{R}_0}\left(\tilde{r}_0\right) = \mathbb{P}\left(\tilde{R}_0 < \tilde{r}_0\right) = \mathbb{E}_{\mathcal{N}}\left[\mathbb{P}\left(\tilde{R}_0 < \tilde{r}_0\right) | \mathcal{N} = n\right] \\
&= \sum_{n=0}^{\infty} P_n\left(\mathcal{A}\left(r_{\max}\right)\right) \mathbb{P}\left(\min_n \left\{\mathcal{X}_n^{-\frac{1}{\alpha}} R_n^{\rm vis}\right\} < \tilde{r}_0\right) \\
&= \sum_{n=0}^{\infty} P_n\left(\mathcal{A}\left(r_{\max}\right)\right) \\
&\times \left(1 - \mathbb{P}\left(\mathcal{X}_1{}^{-\frac{1}{\alpha}} R_1^{\rm vis} > \tilde{r}_0, \cdots, \mathcal{X}_n{}^{-\frac{1}{\alpha}} R_n^{\rm vis} > \tilde{r}_0\right)\right) \\
&\overset{(a)}{=} \sum_{n=0}^{\infty} P_n\left(\mathcal{A}\left(r_{\max}\right)\right)\left(1 - \left(1 - F_{\tilde{R}_n}\left(\tilde{r}_0\right)\right)^n\right), \qquad (17)
\end{aligned}
$$

where $\tilde{R}_n = \mathcal{X}_n{}^{-\frac{1}{\alpha}} R_n^{\rm vis}$ and (a) follows from $\{\tilde{R}_n\}$ being i.i.d. random variables. Since each $\tilde{R}_n$ is the product of independent random variables $R_n^{\rm vis}$ and $\mathcal{Z}_n \triangleq \mathcal{X}_n^{-\frac{1}{\alpha}}$, the product distribution is given by

$$
F_{\tilde{R}_n}\left(\tilde{r}_0\right) = \int_0^{\infty} f_{Z_n}\left(z_n\right) F_{R_n^{\rm vis}}\left(\frac{\tilde{r}_0}{z_n}\right) d_{z_n}. \qquad (18)
$$

Substituting $f_{Z_n}\left(z_n\right) = \alpha z_n^{-\alpha-1} f_{\mathcal{X}_n}\left(z_n^{-\alpha}\right)$ and taking the derivative with respect to $\tilde{r}_0$, the CDF of $\tilde{R}_0$ is obtained as given in Lemma 2.

Acknowledgment

This research work was supported by a Nokia University Donation.

References

[1] N. Okati, T. Riihonen, D. Korpi, I. Angervuori, and R. Wichman, "Downlink coverage and rate analysis of low Earth orbit satellite constellations using stochastic geometry," *IEEE Transactions on Communications*, vol. 68, no. 8, pp. 5120–5134, Aug. 2020.

[2] N. Okati and T. Riihonen, "Stochastic analysis of satellite broadband by mega-constellations with inclined LEOs," in *Proc. IEEE 31st Annual International Symposium on Personal, Indoor and Mobile Radio Communications*, Sep. 2020.

[3] ——, "Modeling and analysis of LEO mega-constellations as nonhomogeneous Poisson point processes," in *Proc. IEEE 93rd Vehicular Technology Conference*, Apr. 2021.

[4] ——, "Nonhomogeneous stochastic geometry analysis of massive LEO communication constellations," *IEEE Transactions on Communications*, Jan. 2022, early access.

[5] A. Al-Hourani, "An analytic approach for modeling the coverage performance of dense satellite networks," *IEEE Wireless Communications Letters*, vol. 10, no. 4, pp. 897–901, Apr. 2021.

[6] ——, "Optimal satellite constellation altitude for maximal coverage," *IEEE Wireless Communications Letters*, vol. 10, no. 7, pp. 1444–1448, Mar. 2021.

[7] A. Yastrebova *et al.*, "Theoretical and simulation-based analysis of terrestrial interference to LEO satellite uplinks," in *Proc. IEEE Global Communications Conference*, Dec. 2020.

[8] A. Talgat, M. A. Kishk, and M.-S. Alouini, "Nearest neighbor and contact distance distribution for binomial point process on spherical surfaces," *IEEE Communications Letters*, vol. 24, no. 12, pp. 2659–2663, Dec. 2020.

[9] ——, "Stochastic geometry-based analysis of LEO satellite communication systems," *IEEE Communications Letters*, vol. 25, no. 8, pp. 2458–2462, Aug. 2021.

[10] H. Lin *et al.*, "Fine-grained analysis on downlink LEO satellite-terrestrial mmWave relay networks," *IEEE Wireless Communications Letters*, vol. 10, no. 9, pp. 1871–1875, May 2021.

[11] M. Mühleisen and B. Walke, "Analytical evaluation of LTE uplink performance in the IMT-Advanced Indoor Hotspot scenario," in *Proc. IEEE 22nd International Symposium on Personal, Indoor and Mobile Radio Communications*, Sep. 2011.

[12] H. S. Dhillon and J. G. Andrews, "Downlink rate distribution in heterogeneous cellular networks under generalized cell selection," *IEEE Wireless Communications Letters*, vol. 3, no. 1, pp. 42–45, Nov. 2014.

[13] D. Ohmann, A. Awada, I. Viering, M. Simsek, and G. P. Fettweis, "Best server SINR models for single- and multi-point transmission in wireless networks," in *Proc. IEEE Global Communications Conference*, Dec. 2015.

[14] F. Vatalaro, G. E. Corazza, C. Caini, and C. Ferrarelli, "Analysis of LEO, MEO, and GEO global mobile satellite systems in the presence of interference and fading," *IEEE Journal on Selected Areas in Communications*, vol. 13, no. 2, pp. 291–300, Feb. 1995.

[15] A. Ganz, Y. Gong, and B. Li, "Performance study of low Earth-orbit satellite systems," *IEEE Transactions on Communications*, vol. 42, no. 234, pp. 1866–1871, Feb. 1994.

[16] H. M. Mourad, A. A. M. Al-Bassiouni, S. S. Emam, and E. K. Al-Hussaini, "Generalized performance evaluation of low Earth orbit satellite systems," *IEEE Communications Letters*, vol. 5, no. 10, pp. 405–407, Oct. 2001.

[17] X. Lu, M. Salehi, M. Haenggi, E. Hossain, and H. Jiang, "Stochastic geometry analysis of spatial-temporal performance in wireless networks: A tutorial," *IEEE Communications Surveys and Tutorials*, Aug. 2021.

[18] M. Haenggi, *Stochastic geometry for wireless networks*. Cambridge University Press, 2012.

[19] B. Błaszczyszyn *et al.*, *Stochastic geometry analysis of cellular networks*. Cambridge University Press, 2018.

[20] J. G. Andrews, F. Baccelli, and R. K. Ganti, "A tractable approach to coverage and rate in cellular networks," *IEEE Transactions on Communications*, vol. 59, no. 11, pp. 3122–3134, Nov. 2011.

[21] H. S. Dhillon, R. K. Ganti, F. Baccelli, and J. G. Andrews, "Modeling and analysis of K-tier downlink heterogeneous cellular networks," *IEEE Journal on Selected Areas in Communications*, vol. 30, no. 3, pp. 550–560, Apr. 2012.

[22] V. V. Chetlur and H. S. Dhillon, "Downlink coverage analysis for a finite 3-D wireless network of unmanned aerial vehicles," *IEEE Transactions on Communications*, vol. 65, no. 10, pp. 4543–4558, Oct. 2017.